

OFDM LOW COMPLEXITY CHANNEL ESTIMATION USING TIME-FREQUENCY ADJUSTABLE WINDOW FUNCTIONS

UDC ((004.3/.4+629.783):517.518.5)

Veljko Stanković, Zoran Perić

University of Niš, Faculty of Electronic Engineering, Department of Telecommunications,
Republic of Serbia

Abstract. *In this paper, we introduce a low complexity algorithm for estimation of the channel transfer function in the OFDM communication system that is using a scattered pilot symbol grid. Although, the use of the scattered pilot grid enables implementation of the flexible, and adaptive radio interface, it suffers from a high estimation error at the edges of the symbol sequence. Due to the sampling in time, and frequency, the signal is circularly expanded in both domains, and this has to be taken into account when the signal is processed. The proposed algorithm is shaping the pilot symbol estimates in time, and frequency domain, such that the aliasing in both domains are reduced or eliminated. We achieve a significant reduction of the estimation error, with a linear increase in computational complexity.*

Key words: *Channel estimation, window functions, signal processing, Discrete Fourier transform*

1. INTRODUCTION

Modern communication systems require accurate channel state information estimates in order to perform a coherent detection that is needed to achieve high data rates. Both the orthogonal frequency division multiplexing (OFDM), and the single carrier with frequency domain equalization (SC-FDE) require accurate and reliable estimates of the channel transfer function (CTF) that can be obtained using known pilot-symbols at the price of a reduced spectral efficiency. The pilot-symbol aided CTF estimation (PACE) is important because it enables us to separate the estimation process from other physical layer functions such as the modulation and coding scheme (MCS) choice or resource allocation. A sophisticated pilot design should achieve a trade-off between the attainable accuracy of the channel estimate and

Received August 24, 2022 / Accepted October 07, 2022

Corresponding author: Veljko Stanković

University of Niš, Faculty of Electronic Engineering, Department of Telecommunications, Aleksandra Medvedeva 14,
18000 Niš, Republic of Serbia

E-mail: veljkost@gmail.com

the bandwidth efficiency in terms of the pilot overhead. These requirements are achieved in certain scenarios by using a scattered pilot grid, where pilot symbols are equidistantly spaced in time and frequency. It facilitates a flexible and adaptive air interface pilot aided channel estimation.

Pilot symbols are scattered in time and frequency such that the Nyquist sampling criterion is satisfied. The interpolation over pilot symbols suffers from the edge effect, where the estimation error significantly increases near the edges of a sequence to be estimated. It is particularly the case near the beginning and at the end of a frame in time, as well as for the subcarriers at the edges of the frequency bandwidth. An estimate of CTF for data subcarriers is obtained by the interpolation between pilot symbols.

The optimum solution for PACE is given by the Wiener interpolation filter [1], [2]. However, an optimum Wiener interpolation filter may be too complex for a practical implementation, because of large dimensions, and the requirement of the channel statistics knowledge. The computation of the filter coefficients in real time has a significant computational load. The computational complexity of the optimum Wiener interpolation filter can be reduced by reducing the dimension and by matching the model to a typical worst case scenario, so the filter coefficients can be precomputed and stored, [3]. A CTF interpolation that is based on the discrete Fourier transform (DFT) is computationally more efficient [4]. The DFT interpolation can be performed very efficiently by two successive DFTs and zero padding. In this case, we rely on the fact that the channel impulse response (CIR) in the time domain is time limited, and that the CIR components are mutually uncorrelated. Unfortunately, since the relative time delay between the CIR components is an exponential random variable, and CIR components are not equally spaced, after DFT of the frequency domain samples, there will be a leakage, and aliasing between the CIR components. The aliasing between the CIR components results in a mean-squared-error (MSE) floor that is much higher than that for the Wiener interpolation. The DFT interpolation MSE error floor is reduced by additional processing using the window function in the frequency domain, and by placing pilot symbols at the first, and at the last subcarrier. Additionally, in [1] the authors use the Wiener filtering in the time domain to reduce the aliasing, which unfortunately requires the knowledge of the CIR statistics, and assumes unrealistically that the CIR components are equally spaced. The same model mismatch is used in [5] to improve the performance of the DFT interpolation, and reduce the edge MSE by extrapolating the pilot tones into the guard bands by using the Wiener filter. Model mismatch assumes a worst case uniform power delay profile with maximum time delay spread. The estimator in [5] significantly reduces the MSE error floor, and at medium signal-to-noise ratios (SNRs) achieves the same performance as the optimum Wiener interpolation filter. Recently, there have been several proposals to use deep neural networks for the CTF estimation. In [12], the time-frequency grid of the channel response is modeled as a two-dimensional image which is known only at the pilot positions. This channel grid with several pilots is considered as a low-resolution image and the estimated channel as a high-resolution one. In the first step, an image super-resolution algorithm is used to enhance the resolution of the low-resolution input. Secondly, an image restoration method is utilized to remove the noise effects. The resulting algorithm does not achieve the MSE of the Wiener interpolation filter, and its performance is highly dependent on SNR at which the neural network is trained.

The CTF estimation error can be separated into two components [6]. The first component depends on the additive noise, and it dominates at low SNRs. As SNR increases, the CTF estimation error linearly reduces. The interpolation error, on the other hand, is independent of

SNR. At high SNRs, the CTF estimation error is dominated by the interpolation error that results in the MSE floor. Unfortunately, both the additive noise, and interpolation error are dependent on the subcarrier index. In particular, near the beginning and at the end of the sequence edge effects result in an increased estimation error.

In this paper we will introduce the DFT based interpolation, that does not rely on the mismatch model, and does not use computationally more demanding Wiener filtering. We rely on the characteristics of the process of the CTF bandlimiting, and sampled signal characteristics in time, and frequency domain in order to significantly reduce or even eliminate the edge effect, and consequently the MSE floor, by using the appropriate window functions (WF) in time, and frequency domain. Our goal is to achieve the estimation performance that is the same or close to the Wiener interpolation filter, with the computational complexity that is same or comparable to the DFT interpolation, and without any mismatch or channel statistics assumptions.

This paper is organized as follows. In Section 2, the system model is described. The CTF interpolation algorithm is presented in Section 3. In Section 4 we present the numerical results, and in Section 5 we give our conclusions.

2. SYSTEM MODEL

Consider an OFDM system where symbols are generated by using an N -point DFT, with N_c subcarriers that are used for the transmission, and N_g subcarriers in the guard bands at the signal bandwidth edges. Assuming perfect timing and frequency offset synchronization, the received signal of subcarrier n of the OFDM symbol is given by:

$$y_n = h_{f,n}x_n + v_n, \quad (1)$$

where $0 \leq n \leq N-1$, x_n is the symbol transmitted on the n -th subcarrier, v_n is the sample of the additive white Gaussian noise on the n -th subcarrier. We assume that v_n are zero mean, complex Gaussian random variables with variance σ_v^2 . If we assume that the CIR has K components, with exponential power delay profile, then

$$h_{f,n} = \sum_{k=1}^{N_{cir}} h_k e^{-j\frac{2\pi}{N}n\tau_k}, \quad (2)$$

where h_k is the k -th CIR component, with time delay τ_k that is normalized to the sampling time T_0/N . OFDM symbol duration is denoted as T_0 .

We assume that the first, and the last N_g subcarriers are in the guard band, and that the maximum time delay spread $\tau_{N_{cir}}$ is less than or equal to the OFDM cyclic prefix with N_{cp} samples. In order to satisfy the Nyquist sampling criterion, the number of the pilot subcarriers N_p should be at least $2N_{cp}$, [6]. Spacing between the pilot symbols is equal to N/N_p . We assume that the first, and the last subcarrier are known pilot symbols.

3. TIME-FREQUENCY WINDOWED DFT INTERPOLATION

By taking the N -point DFT of the sequence that is given in (2), we obtain the time domain samples of the CIR as:

$$h_{f,m} = \frac{1}{\sqrt{N}} \sum_{n=0}^{N-1} h_{f,n} e^{j\frac{2\pi}{N}nm}, \quad (3)$$

which can be shown from (2) to be equal to:

$$h_{f,m} = \frac{1}{\sqrt{N}} \sum_{k=1}^{N_{cir}} h_k \sum_{n=0}^{N-1} e^{-j\frac{2\pi}{N}n(\tau_k-m)}, \quad (4)$$

which actually represents the sampled sequence of the convolution between the CIR, and a function:

$$\frac{1}{\sqrt{N}} \sum_{n=0}^{N-1} e^{-j\frac{2\pi}{N}n(\tau_k-m)} = \frac{1}{\sqrt{N}} \frac{1 - e^{-j2\pi(\tau_k-m)}}{1 - e^{-j\frac{2\pi}{N}(\tau_k-m)}}, \quad (5)$$

that is infinite, and results in component aliasing. By taking N samples of the CTF we have introduced a limit to the time domain estimation resolution, and performed a circular expansion of the CTF in the frequency domain, and of the CIR in the time domain. The edge effect is the result of our attempt to estimate samples of aperiodic functions, based on their circular expansions. In order to reduce the edge effect, and the MSE floor we need to eliminate or reduce the effects of the circular expansion of the CTF, and the CIR.

We will achieve this by taking several steps before interpolation. In the frequency domain we will use a flat-top WF to select the N -sample signal, and the edge subcarriers will no longer sharply change, but gradually go to zero. Next, we will add a sequence of N zeros in order to reduce aliasing in the frequency domain the will result from the processing in the time domain. Since our aim is not to estimate the exact values of the CIR components h_k , and their corresponding delays τ_k , before DFT we will multiply the sequence $h_{f,n}$ with the WF that should have such properties to reduce the time domain aliasing as much as possible. That is, WF should provide as low as possible the peak side-lobe level (PSL) relative to the main-lobe, and the asymptotic side-lobe attenuation (ASA). However, after the interpolation we will need to remove the effect of this WF, and therefore at the edges the value of this WF should be greater than zero in order to avoid significant noise amplification. This limits the ASA of WF to -6 dB/oct. This approach has already been proposed in the literature, but with different optimization parameters of WF, [5], [7], whereas in [1], anti-aliasing is performed directly, and only in the time domain. After we transform the signal to the time domain, we will first find the minimum point of the CIR aliasing due to its circular expansion, and smooth the transition between the circularly expanded parts of CIR in order to reduce the aliasing, and the estimation error in the frequency domain after the interpolation. The per-processing in the frequency domain is shown in Fig. 1, and the time domain processing in Fig. 2.

Signal selection WF, $w_{sel}(n)$ is equal to one for $n = N_{ws}, \dots, N - N_{ws} - 1$, and for $n = 0, \dots, N_{ws} - 1$, and $n = N - N_{ws}, \dots, N - 1$ it is equal to $w_a(n)$ that has desirable PSL, and ASA. From Fig.1 we can see that N_{ws} can be chosen to be greater than the guard band width in order to achieve better spectral properties. The rationale is that this part of the frequency domain sequence is the one that is most affected by the edge effect, and that therefore some

attenuation is acceptable if we can achieve lower estimation MSE. In general, we choose $w_a(n)$ such that for $n > N_g$, the subcarrier attenuation is not greater than 2dB. After interpolation, we will have some values for subcarriers in the guard bands, but these values are in general discarded. After multiplying the CTF samples with the selection WF, we add a sequence of N zero samples. Zero padding of the sequence of CTF samples has two effects. First, we reduce the aliasing in the frequency domain that results from time domain processing, and circular expansion in the frequency domain. Second, by zero padding we double the sampling rate in the time domain. We could further increase the sampling rate, but it does not provide any additional gains, while it increases the computational load.

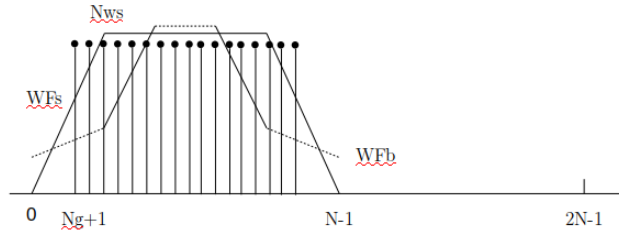


Fig. 1 Frequency domain signal selection using WF, and zero padding.

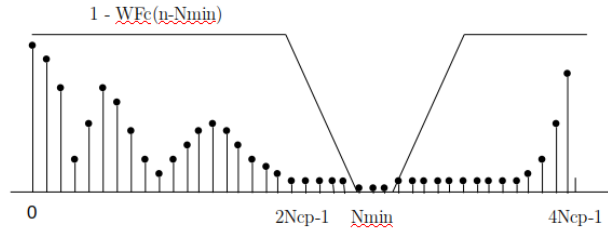


Fig. 2 Time domain signal spectral shaping using WF, and zero padding.

Let us denote a sequence of CTF samples on the pilot subcarriers as:

$$h_{f,p} = \hat{h}_{f, N_g + 1 + pN/N_p}, \quad (6)$$

$p = 0, \dots, N_p - 1$, where

$$\hat{h}_{f,n} = h_{f,n} w_b(n), \quad (7)$$

are the filtered CTF samples using the second type of WF that is characterized by low spectral leakage, and minimum aliasing in time domain. Sample parameters are chosen such that the first and the last subcarrier are pilot subcarriers. If we introduce the following vectors of CTF samples:

$$\mathbf{h}_f = [h_{f,0} \cdots h_{f,N-1}]^T, \quad (8)$$

The vector of WF that is used for the time domain spectral shaping:

$$\mathbf{w}_b = [w_{b,0} \cdots w_{b,N-1}]^T, \quad (9)$$

we can write:

$$\hat{\mathbf{h}}_f = [\mathbf{h}_f \otimes \mathbf{w}_b; \mathbf{0}_N] \in \mathbb{C}^{2N \times 1}, \quad (10)$$

where \otimes denotes the Haddamard matrix product. Let us denote a vector of CTF samples only on the pilot subcarriers of $\hat{\mathbf{h}}_f$ as $\hat{\mathbf{h}}_{f,p}$, then we can write that:

$$\hat{\mathbf{h}}_{t,p} = \mathbf{F}_{2N_p}^H \hat{\mathbf{h}}_{f,p}, \quad (11)$$

where $\hat{\mathbf{h}}_{t,p}$ denotes the vector of CIR samples in the time domain of size $2N_p \times 1$. The $2N_p$ -point DFT matrix is denoted as \mathbf{F}_{2N_p} .

Next, we search for the point in the second half of the vector $\hat{\mathbf{h}}_{t,p}$ that has minimum envelope, and expand the length of the pilot CIR to $2N$:

$$N_{\min} = \min \hat{\mathbf{h}}_{t,p}(N_p : 2N_p), \quad (12)$$

where $\mathbf{a}(i:j)$ denotes the range of elements of a vector that are used for optimization. Spectral shaping in the frequency domain is performed by:

$$\tilde{\mathbf{h}}_{t,p} = \hat{\mathbf{h}}_{t,p} \otimes (1 - \mathbf{w}_c (>> N_{\min})), \quad (13)$$

where WF $\mathbf{w}_c (>> N_{\min})$ denotes WF \mathbf{w}_c that is shifted to the right by N_{\min} samples. Choice of \mathbf{w}_c will influence interpolation of the CTF samples between the pilot CTF samples, and the spectral leakage in the frequency domain. Finally, at N_{\min} position of $\tilde{\mathbf{h}}_{t,p}$ we add $2N - 2N_p$ zeros:

$$\bar{\mathbf{h}}_t = [\tilde{\mathbf{h}}_{t,p}(1 : N_{\min}); \mathbf{0}_{2(N-N_p)}; \tilde{\mathbf{h}}_{t,p}(N_{\min} + 1 : 2N_p)], \quad (14)$$

where $\mathbf{0}_M$ denotes all zero element vector of size $M \times 1$.

Finally, we interpolate CTF by taking DFT:

$$\bar{\mathbf{h}}_f = \mathbf{F}_{2N} \bar{\mathbf{h}}_t, \quad (15)$$

and by taking only the first N samples, and compensate for the time domain spectral shaping WF \mathbf{w}_b , we obtain the interpolated CTF:

$$\tilde{\mathbf{h}}_f = \bar{\mathbf{h}}_f(1 : N) \otimes \mathbf{w}_b^{-1}. \quad (16)$$

The proposed time-frequency spectral shaping DFT interpolation has a slightly higher computational load in comparison to the regular DFT interpolation, because it requires two DFT operations at two times more points, $2N_p$, and $2N$, and one additional vector multiplication with the selection WF.

4. NUMERICAL RESULTS

Performance of the DFT interpolation with time-frequency spectral shaping will depend on the choice of the parameters of WFs that are used for specific goals. In order to be flexible, and able to fine tune specific parameters of each WF that is used, we will use the adjustable WF that provide us with the possibility to choose all the parameters that influence resolution, and spectral leakage, [8]. The adjustable WFs that are proposed

in [9] are based on ultraspherical polynomials, and also allow us to adjust the WF parameters depending on the required spectral properties. However, it has been shown that WFs proposed in [8] result in lower main-lobe width, because side-lobes near the main-lobe have in some parts constant amplitude. The Dolph-Chebyshev WF does have the lowest main lobe width. However, the first and the last sample of its impulse response are much higher, which results in undesirable response averaging, and it is therefore rarely used in practice, [8].

All of the WFs that are used in this paper are obtained iteratively as [8]:

$$w_m(n) = \beta_m w_{m-1}(n) + (1 - \beta_m) w_H^{\alpha+m+\Delta_m}(n), \quad (17)$$

where $n = 0, \dots, N_w - 1$, N_w , is the length of the WF, and the real valued parameters $\alpha \geq 0$, $0 \leq \beta_m \leq 1$, Δ_m , and $\Delta_0 = 0$ control the spectral properties of the WF. WF $w_H(n)$ denotes the Hann WF:

$$w_0(n) = w_H(n) = \left(\frac{\pi}{N_w} n \right)^2. \quad (18)$$

In our simulations we will use WFs with the following parameters:

- 1) \mathbf{w}_a : $m = 1$, $\alpha = 0.34$, $\beta_1 = 1$, $\Delta_1 = 1$, $N_w = 38$,
- 2) \mathbf{w}_b : $m = 3$, $\alpha = 0$, $\boldsymbol{\beta} = [0.26 \quad 0.221 \quad 0.742]$, $\boldsymbol{\Delta} = [0.818 \quad 0.072 \quad 0.92]$, $N_w = N$,
- 3) \mathbf{w}_c : $m = 1$, $\alpha = 0.34$, $\beta_1 = 1$, $\Delta_1 = 1$, $N_w = 9$,

Chosen WFs have the following spectral properties. WF that is used to select signal in the frequency domain \mathbf{w}_a , has PSL of -20dB, ASA of -10dB/oct, and variable window length of $N_w / 2 = 19$. WF that is used for spectral shaping in the time domain \mathbf{w}_b , has PSL of -20dB, and ASA of -6dB/oct, while its window length will vary depending on the specific length of the sequence in the frequency domain. The last WF \mathbf{w}_c , that is used for spectral shaping in the frequency domain has also PSL of -20dB, ASA of -10dB/oct, and the window length of $N_w = 9$.

The parameters of \mathbf{w}_a are chosen so that in our simulations it does not span more than three pilot subcarriers on each side of the signal bandwidth, and that the maximum attenuation in this range does not exceed more than 2dB. These subcarriers are only a couple of percents of the total number of subcarriers, and by shaping this part of the useful spectrum helps us reduce the edge MSE on one hand, with the acceptable loss that can be compensated by using the forward error correction coding over all subcarriers, including the majority that will have much lower CTF estimation error. Parameters of the second WF, \mathbf{w}_b , are chosen such to have the spectral leakage as low as possible. We gave priority to minimizing the PSL because we needed to minimize the aliasing between the neighboring CIR components, especially the first, and the last one. By padding the sequence in the frequency domain with N zeros, we are more flexible with the choice of the WF \mathbf{w}_c . Its parameters are chosen as a compromise between the minimum main-lobe width, and the ASA. These two parameters are inversely proportional, and as ASA decreases, resulting in lower spectral leakage, the main-lobe width increases, which results in lower frequency resolution. The main lobe of the chosen WF is only slightly greater than the main-lobe width of the rectangular WF, but has lower ASA by -4dB/oct that is enough considering the number of padded zeros in the frequency domain. We note that in a conventional DFT interpolation, the time domain processing is performed by using rectangular WF \mathbf{w}_c , which results in large spectral leakage at bandwidth edges.

In our simulations we have set that the cyclic prefix (CP) of the OFDM symbol is $N_{cp} = 16$. In order to satisfy the Nyquist sampling criterion, we set $N_p = 32$. First, we will compare the performance of the conventional DFT interpolation, and the proposed time-frequency DFT interpolation for $N = 320$. In case of conventional DFT we set that $N_{min} = N_p / 2$, and that no WF are used. Next, for comparison we use the case of the conventional DFT when we use the same WF to select the signal in the frequency domain as in the case of our proposed algorithm. This algorithm is denoted as conWDFT.

CIR is modeled with exponential power delay profile. Number of CIR components has the Poisson distribution, and the time delay between the CIR components is exponentially distributed, [10], [11]. Maximum power attenuation is set to -25dB. CIR is normalized so that the average power of the CTF sample is equal to one. SNR is defined as the ratio of the average CTF sample power, and additive noise variance.

In Fig. 3. we compare three algorithms for CTF interpolation when the maximum time delay of the CIR is equal to the CP time interval. Simple frequency domain shaping of the bandwidth edges provides addition 5dB MSE reduction with respect to the conventional DFT. The proposed spectral shaping using WFs in both time, and frequency domain provides more than 12 dB gain over the conventional DFT interpolation.

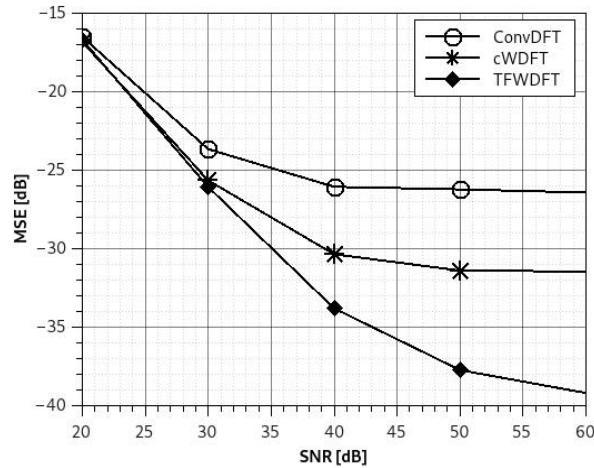


Fig. 3 MSE comparison for $T_m = T_{cp}$.

Case when the channel time delay spread is equal to CP is a worst case scenario. Very often it is much shorter than CP. In Fig. 4. we compare the same algorithms when the channel time delay spread is 80%, 60%, and 40% of CP, $T_m = 0.8 T_{cp}$, $T_m = 0.6 T_{cp}$, and $T_m = 0.4 T_{cp}$.

In this case, the DFT interpolation with frequency domain shaping has 7dB gain over the conventional DFT interpolation, whose performance has not changed.

Finally, in Fig. 5. we compare MSE of the various algorithms as a function of the number of samples in the frequency domain for $SNR = -80$ dB, and $T_m = 0.6 T_{cp}$. As this number decreases, and with all other parameters fixed, the result is that the number of subcarriers between the pilot subcarriers also reduces. This has an effect only on the conventional DFT with the frequency domain WF selection, MSE significantly reduces. Performance

of the conventional DFT interpolation does not change with the time delay spread of CIR, or the spacing between the pilot subcarriers.

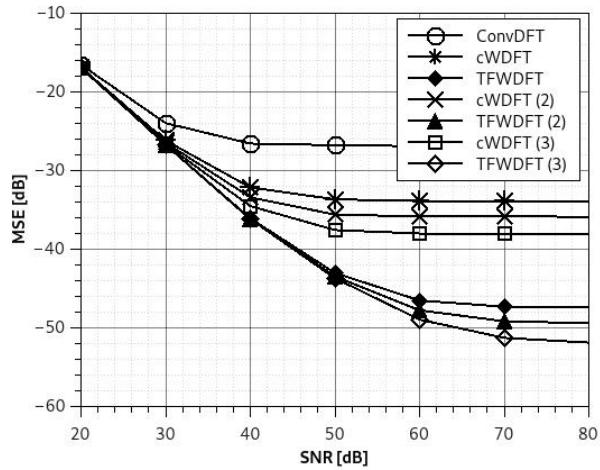


Fig. 4 MSE comparison for $T_m = 0.8T_{cp}$, (2) $T_m = 0.6T_{cp}$, and (3) $T_m = 0.4T_{cp}$.

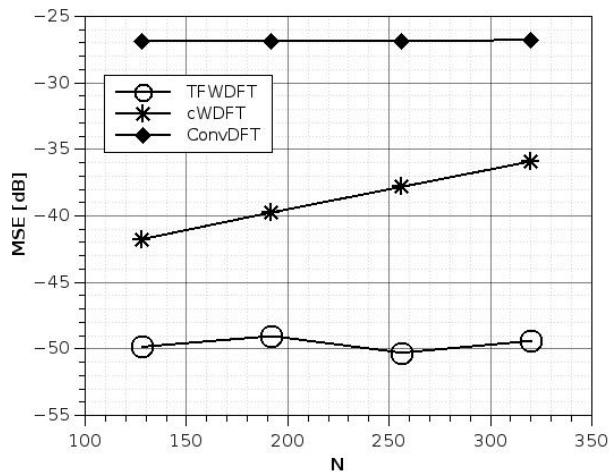


Fig. 5 MSE as a function of N, SNR = -80dB.

The algorithm that is proposed in this paper does not eliminate the edge effect. However, as a result of zero padding, and by using the first flat-top WF to select the sequence in the frequency domain, we significantly reduce the interpolation error, and the number of the subcarriers at the edges that are affected, in comparison to the conventional DFT interpolation or cWDFT. Overall, the interpolation error for TFWDFT in the middle of the bandwidth is significantly reduced to the point that at the high SNRs it is several orders of magnitude lower and almost negligible.

Computational complexity of the proposed algorithm TFWDFT, is two times higher than the complexity of cWDFT. However, it does achieve the MSE of the Wiener interpolation filter, and has a much lower MSE floor. However, its complexity is much lower than that of the Wiener interpolation filter which is a square function of the number of the subcarriers.

7. CONCLUSION

In this paper, we have introduced a novel low complexity channel estimation algorithm that is using DFT interpolation and the signal spectral shaping in time, and frequency domains in order to reduce the error floor that is characteristic for CTF estimation based on scattered pilot grid. We avoid using any worst case assumptions or Wiener filtering that requires the matrix inversion, and knowledge of the channel statistics. The spectral shaping is achieved using adaptive WFs that enable us to fine tune their parameters in order to meet a specific criterion. Depending on the length of CIR, the novel interpolation algorithm can achieve significant gains relative to other low complexity proposals.

Acknowledgement: *This work has been supported by the Ministry of Education, Science and Technological Development of the Republic of Serbia.*

REFERENCES

- [1] G. Auer, S. Sand, A. Dammann, "Comparison of Low Complexity OFDM Channel Estimation Techniques", In: *Proc. of Int. OFDM Workshop*. 2003.
- [2] G. Auer and E. Karipidis, "Pilot aided channel estimation for OFDM: a separated approach for smoothing and interpolation," in Proc. IEEE ICC'2005, vol. 4, pp. 2173-2178, May 2005. doi: 10.1109/ICC.2005.1494722
- [3] P. Hoeher, S. Kaiser, and P. Robertson, "Pilot-Symbol-Aided Channel Estimation in Time and Frequency," in Proc. Communication Theory Mini-Conf. (CTMC) within IEEE Global Telecommun. Conf. (GLOBECOM'97), Phoenix, USA, pp. 90–96, 1997. doi: 10.1007/978-1-4615-6231-3_20
- [4] B. Yang, Z. Cao, and K. B. Letaief, "Analysis of low-complexity windowed DFT-based MMSE channel estimator for OFDM systems," *IEEE Trans. Commun.*, vol. 49, no. 11, pp. 1977-1987, Nov. 2001. doi: 10.1109/26.966074
- [5] J.W. Seo et al., "An enhanced DFT-based channel estimation using virtual interpolation with guard bands prediction for OFDM", in Proc.PIMRS06, 2006. doi: 10.1109/PIMRC.2006.254263
- [6] D2.1 Identification of Radio-link technologies, Technical report, IST-2003-507581 WINNER
- [7] AJ van-der Veen, M.C. Vanderveen, A. Paulraj, "Joint angle and delay estimation using shift-invariance techniques", *IEEE Trans. on Sig. Proc.*, vol.46, No 2, February 1998. doi: 10.1109/78.655425
- [8] V. Stankovic, "Adjustable high resolution window function", *El. Lett.*, vol 54, No 13, p. 827-829, June 2018. DOI: 10.1049/el.2018.0448
- [9] S.W.A Bergen, A. Antoniou: 'Design of ultraspherical window functions with prescribed spectral characteristics', *EURASIP J. Appl. Signal Process.*, vol 2004, No 1, pp. 2053–2064, 2004 doi: 10.1155/S1110865704403114
- [10] A. A. M. Saleh and R. A. Valenzuela, "A statistical model for indoor multipath propagation," *IEEE J. Sel. Areas Commun.*, vol. SAC-5, pp.128–137, Feb. 1987. doi: 10.1109/JSAC.1987.1146527
- [11] Meijerink, A., & Molisch, A. F. (2014). On the physical interpretation of the Saleh–Valenzuela model and the definition of its power delay profiles. *IEEE Transactions on Antennas and Propagation*, 62(9), 4780-4793. doi: 10.1109/TAP.2014.2335812
- [12] S. Mehran, et al. "Deep learning-based channel estimation." *IEEE Communications Letters* vol 23, No. 4, p. 652-655. April 2019. doi: 10.1109/LCOMM.2019.2898944